

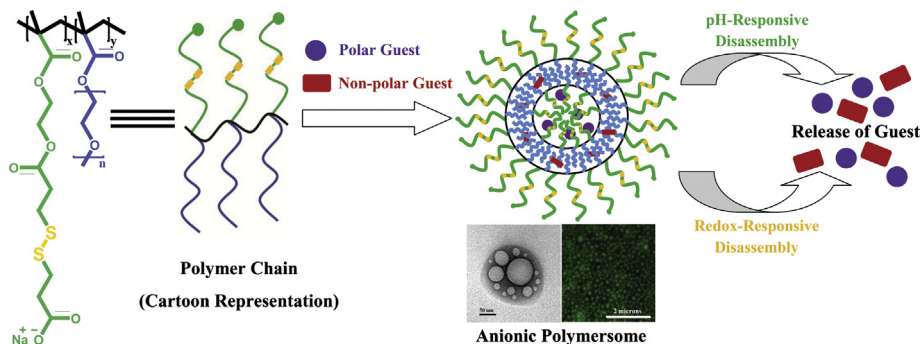


Regular Article

Spontaneously formed redox- and pH-sensitive polymersomes by mPEG based cytocompatible random copolymers

Partha Laskar^a, Joykrishna Dey^{a,*}, Sudip Kumar Ghosh^b^a Department of Chemistry, Indian Institute of Technology Kharagpur, 721 302, India^b Department of Biotechnology, Indian Institute of Technology Kharagpur, 721 302, India

GRAPHICAL ABSTRACT



ARTICLE INFO

Article history:

Received 19 February 2017

Revised 9 April 2017

Accepted 10 April 2017

Available online 12 April 2017

Keywords:

Random copolymers

Anionic polymersomes

Redox- and pH-responsiveness

PEG

Cytocompatible

Hemocompatible

ABSTRACT

Stimuli-sensitive polymersomes are one of the important vehicles and have been extensively studied as smart drug delivery system. Polymersomes have added advantage over the micelles because of having the ability to carry not only hydrophobic but also hydrophilic guest in their aqueous core. Among various stimuli, the change of pH and redox reaction is very important for drug delivery purpose especially for anticancer drug. Therefore, in this work, two poly(ethylene glycol) methyl ether methacrylate (mPEG) containing hydrophilic random anionic copolymers, poly[(2-hydroxyethyl methacrylate-3,3'-dithiodipropionic acid)_x-co-(poly(ethylene glycol) methyl ether methacrylate)_y], poly[(HEMA-DTDPA)_x-co-mPEG_y] with different copolymer ratios were designed and synthesized. The self-assembly behaviour of these copolymers were studied by use of various techniques, including fluorescence spectroscopy, light scattering, and electron and optical microscopy. Both the copolymers were observed to form negatively charged polymersomes spontaneously in aqueous media at pH 7. The polymersomes were shown to successfully encapsulate hydrophobic as well as hydrophilic guests. The polymersomes of both the polymers showed pH- and redox-sensitive release of encapsulated guest leading to a very good system for cytoplasmic delivery. The polymers were found to be nontoxic and hemocompatible up to a reasonably high concentration. Also the polymers did not show any denaturing effect on the secondary structure of carrier protein, human serum albumin. It was concluded that these two dual stimuli-sensitive cytocompatible polymersomes can have potential use as drug delivery system in cancer chemotherapy.

© 2017 Elsevier Inc. All rights reserved.

* Corresponding author.

E-mail address: joydey@chem.iitkgp.ernet.in (J. Dey).

1. Introduction

Self-assembled polymeric nanostructures are one of the important colloidal systems that are integrated with the advancement of drug delivery and gene transfection [1–4]. Block copolymers can self-assemble to form aggregates of various morphologies, including micelles and vesicles depending upon various structural parameters and way of reactions [5–7]. Polymeric vesicles or polymersomes are such an important kind of self-assembled nanostructures which due to their cell- and virus-mimicking dimensions and functions have potential applications in biotechnology, medicine, pharmacy and even in enzymatic reactions [8–10]. Structurally, in polymersomes, a bilayer consisting of entangled chains separates a fluid-filled core from the bulk medium [11]. Thus polymersomes have an added advantage over polymeric micelles or polymeric nanoparticles in that they can carry hydrophobic as well as hydrophilic cargo within them. The molecular weight of the copolymer generally governs membrane thickness of polymersomes as well as determines their properties such as elasticity, permeability, and mechanical stability [8,12]. Though polymersomes have similar morphology like liposomes, but due to the higher molecular weight of the polymers (more than 10 k) as compared to phospholipids (generally 1 k), the membrane of polymersomes is generally thicker, stronger, tougher and, thus, are inherently more stable than conventional liposomes [13].

In recent years, stimuli-responsive smart polymersomes have become one of the most fascinating subject in drug delivery research and much progress has been made in this direction [14,15]. The most frequently applied stimuli are pH [16,17], temperature [18,19], redox potential [20], magnetic field [21], light [22], ultrasound [23] and enzyme [24]. Among these, pH- and redox- sensitivity have become most appealing internal triggers or stimuli, as they exist naturally in certain pathological sites and/or intracellular compartments [25]. According to the Warburg effect, malignant tumor cells generate most of their energy through glycolysis instead of the normal oxidative phosphorylation, resulting in an acidic environment in the cellular compartment [26]. Also different parts of our body have different pH, so pH can be used as an interesting stimulus to trigger the polymeric drug delivery systems (DDSs) [27]. The pH-sensitive drug carriers can deliver their cargo either via hydrolysis of pH-sensitive bonds (leading to a sustained release of the guest) or swelling and dissociation of protonated groups (leading to a burst release of the guest) [28]. Generally, pH-sensitive polymers are associated with some acidic ($-\text{COOH}$, $-\text{SO}_3\text{H}$) or basic ($-\text{NH}_2$) groups that are ionized in aqueous solution of suitable pH [29–31]. Negatively charged polymers mimicking the RBC cell line (zeta potential = -15 mV) has the advantage of being more stable over time [32]. It is also reported that when the anionic polymers having acidic $-\text{COOH}$ groups are deprotonated at endosomal pHs, their hydrophilicity increases leading to enhanced endosomal membrane disruption. So such kind of pH-dependent membrane disruption and enhanced

endosomal release makes these synthetic pH-sensitive anionic polymers a good choice for drug delivery [33]. On the other hand, redox-sensitive DDSs involving disulfide-thiol chemistry is one of the promising field because disulfide ($-\text{S}-\text{S}-$) linkages in the polymeric nanostructures can be cleaved to the corresponding thiols in presence of reducing agents, specially thiols [33–36]. Glutathione (GSH), a tripeptide containing cysteine, is such a cellular reducing agent for any water soluble DDSs due to presence of free pendant sulfhydryl ($-\text{SH}$) groups [36]. But the concentration of the GSH in intracellular (≈ 10 mM) and extracellular compartments (< 10 μM) of living cells is found to be different [36,37]. Even the tumor tissues are known to have GSH concentration at least 4-fold higher than that of normal tissue in mice [36,37]. The huge difference in GSH concentration between intracellular and extracellular compartments and the further elevated concentration level of GSH in cancer cells in comparison to normal one promotes the thiol-responsive smart polymers as more convenient DDSs [33–39]. Also the pathological signals associated with reactive oxygen species (ROS) for some serious diseases like arteriosclerosis, heart injury and cancer can be exploited as guidance for redox-responsive DDSs [40].

Generally, polymersomes formation is known to occur through self-assembly of block copolymers having a proper ratio of hydrophobic and hydrophilic block [41,42]. Sometimes organic solvent is needed to form the polymersomes [43]. Hydrophilic polymers are also able to form various self-assembled nanostructures including polymersomes, but with the help of external stimuli [44,45]. However, our group recently reported spontaneous polymersome formation from a series of mPEG-based zwitterionic random copolymers (instead of block copolymers) without having any conventional hydrophobe in the polymer chain [46]. So it has become our obvious choice to evaluate mPEG-based cationic [47] as well as anionic random copolymers as DDS instead of these zwitterionic polymersomes. In fact, our group for the first time, reported spontaneous nanostructure (e.g. vesicle and micelle) formation by low-molecular-weight surfactant monomer containing mPEG chain conjugated to a zwitterionic or cationic or anionic head group [48–50]. In continuation with our previous works on these mPEG-based monomeric and polymeric surfactants, presently we aimed to study self-assembly behaviour and evaluate the potential of the more stable self-assembled nanostructure obtained from mPEG-based anionic random copolymers having not only $-\text{COOH}$, but also disulphide bridge in the side chains of the polymer as dual stimuli-sensitive DDS. Accordingly, we have synthesized two novel anionic random polymers poly[(2-hydroxyethyl methacrylate-3,3'-dithiodipropanoic acid) $_x$ -co-(poly(ethylene glycol) methyl ether methacrylate) $_y$], poly[(HEMA-DTDP) $_x$ -co-mPEG $_y$] (**AP12**, $x:y = 1:2$ and **AP14**, $x:y = 1:4$) in which the acidic functionality along with a disulfide linkage and mPEG chains are grafted to their backbone at different ratios (**Chart 1**). The self-assembly behaviour of these anionic polymers (**APs**) were investigated in detail by use of steady-state fluorescence

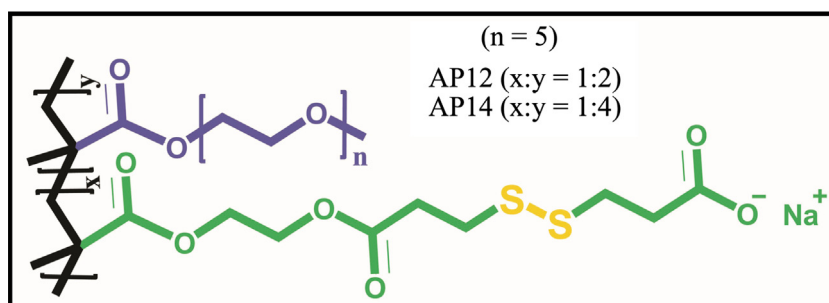


Chart 1. General chemical structure of the anionic polymers **AP12** and **AP14**.

technique using various fluorescent probes. The morphology of the aggregates was determined by electron and optical microscopy along with dynamic light scattering. The surface charge of the aggregates was determined through zeta potential measurements. Both polymers were successfully observed to encapsulate hydrophilic as well as hydrophobic guests in their nanostructure. Their pH-sensitive nature was evidenced by the burst release of hydrophilic cargo, calcein (Cal), from the aggregates. Similarly, their redox-sensitive nature was also studied by fluorescence, electron microscopy and dynamic light scattering techniques. In order to test their suitability for drug delivery applications, cell viability and hemocompatibility measurements were performed.

2. Experimental section

2.1. Materials

Polyethylene glycol methyl ether methacrylate or methoxy poly (ethylene glycol) (mPEG, $M_n \sim 300$), hydroxyethyl methacrylate (HEMA), 3,3'-dithiodipropionic acid (DTDPA), N,N'-dicyclohexylcarbodiimide (DCC), 4-Dimethylamino-pyridine (DMAP), 3-(4,5-dimethylthiazol-2-yl)-2,5-diphenyl-tetrazolium bromide (MTT), chloroform-d were purchased from Sigma-Aldrich (Bangalore, India) and were used without further purification. S-(+)-camptothecin (CPT) was purchased from Tokyo Chemical Industry, Japan. 2, 2'-Azo-bis-(isobutyronitrile) or AIBN was purchased from sigma-Aldrich (Bangalore, India) and used after recrystallization from acetone. All the fluorescent probes, pyrene (Py), N-phenyl-1-naphthyl amine (NPN) and calcein (Cal) were purchased from Sigma-Aldrich (Bangalore, India). Solvents like methanol (MeOH), acetone, tetrahydrofuran (THF), chloroform (CHCl_3), and ethyl acetate, solvents were purchased from Merck, India and were distilled and purified before use. Milli Q (18.2 Mohm cm) water was obtained from Millipore water purifier (Elix, Bangalore, India).

The polymers were synthesized following a procedure already reported by us [46,47,51,52]. The details are available under "Electronic Supporting Information" (ESI).

2.2. General instrumentation

^1H and ^{13}C NMR spectra of the monomer were recorded on 400 MHz NMR spectrometer (AVANCE DAX-400, Bruker, Sweden) using TMS as the internal standard. ^1H NMR spectra of the polymers were recorded using 600 MHz NMR spectrometer (Bruker, Sweden). Electronic/absorption spectra were recorded by use of a UV-vis spectrophotometer (Shimadzu, model UV-2450). The weight average molecular weight (\bar{M}_w) and polydispersity index (PDI) of the copolymers were determined using gel permeation chromatography (GPC, Waters 2414, Refractive Index Detector, 10 Waters 515 HPLC PUMP) using poly(methyl methacrylate) (PMMA) as molecular weight standard. THF (HPLC grade) was used as an eluent at a flow rate of 1 mL/min at 34 °C. The solution pH was measured using a digital pH meter model 5652 (EC India Ltd., Calcutta) using a glass electrode. An electronic digital balance (Sartorius, CP225D) was used to measure the weight of the compounds.

2.3. Surface tension measurement

Du Nuoy ring detachment method was employed for surface tension (γ) measurements of the aqueous copolymer solutions at 25 °C using a semiautomatic surface tensiometer (model 3S,GBX, France). The platinum ring was used after proper cleaning with ethanol/HCl (1:1, v/v) solution and burning in oxidizing flame immediately before every use. For each polymer, the γ value of

water was measured first and then an aliquot from stock of polymer solution was added to it gradually for the surface tension measurements at different polymer concentrations. Before measurement, each sample was equilibrated for 15–20 min. For each concentration, γ value was measured in triplicate and the mean value was noted.

2.4. Fluorescence measurements

Steady-state fluorescence measurements using Py as fluorescent probe were carried out with a SPEX Fluorolog-3 spectrofluorometer (450 WATT 40 ILLUMINATOR, Model: FL-1039/40, HORIBA JOBIN YVON, EDISON, NJ, USA). An aliquot of Py stock solution (1.0×10^{-3} M in MeOH) was taken into 5 mL volumetric flasks and the solvent was evaporated by a continuous stream of N_2 gas. Then polymer solutions in Milli-Q water in different concentrations were added to the volumetric flasks, making the final concentration of Py to 1.0×10^{-6} M. The polymer solutions were equilibrated overnight before measurement. The solutions containing Py probe were excited at 343 nm, and the emission spectra were recorded in the range of 350–600 nm. The excitation and emission slit widths were 5 and 2 nm, respectively. Solutions containing NPN (ca. 1×10^{-6} M) were excited at 340 nm and emission spectra were recorded in the wavelength range 350–550 nm on the SPEX Fluorolog-3 spectrophotometer. Both excitation and emission slit widths were fixed at 5 nm.

2.5. Dynamic light scattering

The hydrodynamic diameter (d_H) of aggregates in aqueous media was measured by conventional dynamic light scattering (DLS) technique using Malvern Nano ZS instrument employing a 4 mW He-Ne laser ($\lambda = 632.8$ nm). All the scattering photons were collected at a 173° scattering angle. The temperature was set to 25 °C and before every measurement each polymer solution was filtered through 0.45 μm filter paper (Millipore Millex syringe filter). The software provided by the supplier calculated d_H using Stokes-Einstein equation.

2.6. Transmission electron microscopy

A high resolution transmission electron microscope (HRTEM, TECNAI G2-20S TWIN, Japan) operating at an accelerating voltage of 200 kV at room temperature was employed to take micrographs of the polymers solutions at a known concentration. A 5 μL aqueous polymer solution was drop cast on a carbon-coated copper grid (400 mesh size) and it was kept in vacuum desiccators overnight for drying.

2.7. Dye encapsulation

For hydrophilic dye encapsulation, a reported procedure was followed [46,47]. An aliquot of the anionic hydrophilic dye (Cal) from the stock solution ($\sim 1 \times 10^{-4}$ M in MeOH) and required amount of the solid polymer were taken in a volumetric flask and then MeOH was evaporated by a stream of dry N_2 gas. The thin film of the polymer thus formed was soaked overnight in 100 μL buffer. The mixture was vortexed (Cyclo Mixer, REMI Equipments, India) for 10 min and then phosphate buffer (pH 7) was added to make up the volume to obtain desired polymer and dye ($\sim 1 \times 10^{-5}$ M) concentration. An 1 mL aliquot of this polymer solution was dialyzed in a double sided Biodialyzer cell (Sigma Aldrich, Bangalore, India) against ~ 100 mL of the same buffer (pH 7) for about 12–15 h with an intermittent change of the external buffer after each 1 h to remove the free dye molecules. This dialyzed solution was used for microscopic as well as for fluorescence

measurements. The dialyzed solution was also used as a stock polymer solution for the study of pH-triggered release of encapsulated dye, if any, in buffers of lower pH. The release was measured by monitoring fluorescence intensity at the emission maximum of the dye molecule.

2.8. Circular dichroism spectra

Interaction of these polymers at different concentrations with blood circulatory protein (HSA) was observed by measuring circular dichroism (CD) spectra in nitrogen atmosphere using spectropolarimeter (JASCO, J-810, Tokyo, Japan) in the far-UV region (190–270 nm) with a Peltier type temperature controller from JASCO attached with the machine. A quartz cell with a path length of 1 mm was used for measurement. 150 W air-cooled xenon lamp was used for this CD machine as a source of light with measurement wavelength range from 163 to 900 nm (standard detector). A fixed amount of HSA (0.1% or 1 g/L or 15 μ M) solution was incubated with different polymer concentration (0.01, 0.05, and 0.1%) for around 24 h before measurement. An average data of two consecutive scans with a scan speed of 50 nm/min was collected for each nm from 270 to 190 nm at an operating temperature of 298 K. CD spectra of the corresponding buffer and polymer concentration were taken as a reference before every measurement and spectra were corrected for buffer signal.

Further, percentage of α -helix content of HSA in native state and in complex with polymer was calculated for better comparison. α -helix (%) were calculated from mean residual ellipticity at 208 nm (MRE_{208}) and corresponding $\theta_{observed}$ in CD spectroscopy using following equations [53–56]:

$$MRE = \theta_{obs}M/(nIC) \quad (1)$$

$$\alpha\text{-helix (\%)} = (-MRE_{208} - 4000)/(33000 - 4000) \quad (2)$$

where θ_{obs} is the CD in millidegrees, M is the molecular weight (66.4 kDa) of the HSA protein in g/dmol, n is the number of the amino acid residues (585 in the case of HSA), l is the path length (1 mm) of the cuvette, and C is the concentration (0.1% or 1 g/L) of the protein in g/L. MRE_{208} is the observed MRE values at 208 nm, 4000 is the MRE of the β -form and random coil conformation cross at 208 nm and 33000 is the MRE value of a pure α -helix at 208 nm.

2.9. Fluorescence microscopy

Fluorescence microscope (Olympus IX 70) was used to visualize the dimensions of the dye entrapped vesicles. Microscope glass slides (Riviera, 25.4 \times 76.2 mm) were treated with a dye entrapped vesicles solution prior to use in order to prevent the vesicles from adhering to the glass coverslip. All the images of vesicles were taken at room temperature and images projections were analyzed using FV10-ASW 1.6 Viewer software.

2.10. Cell cytotoxicity

A conventional and standard MTT dye reduction assay was performed to assess the cell viability or cytotoxicity of the synthesized polymers on HeLa cells [46,47,51,52]. HeLa cells were cultured in DMEM (Dulbecco's Modified Eagle's Medium) supplemented with antibiotics solution containing penicillin (100 units/mL), 10% fetal bovine serum (FBS), amphotericin B (0.25 μ g/mL), and streptomycin (0.1 mg/mL). The cells were incubated with a feeding cycle of 48 h at 310 K in T-25 flasks in a 5% CO₂ humidified chamber. The cells were trypsinized (0.25% Trypsin + 0.1% EDTA) and harvested by centrifugation at 1500 rpm, after sufficient level of confluency in cells monolayer was reached.

For cytotoxicity measurement, the collected cell suspensions were seeded in 200 μ L of complete DMEM in a 96-well plate at a concentration 2×10^3 cells/well further to adhere and grow for nearly 16 h at 310 K in a 5% CO₂ humidified incubator. Polymer stock solutions of definite concentration were prepared in incomplete DMEM medium and after 2 h of incubation the solutions were filtered through 0.2 μ m polycarbonate filter just before addition. Before addition of the polymer solutions, the medium from the cultured cells in each well was carefully removed and a total of 200 μ L of fresh medium containing polymers with the desired concentrations were added for viability measurement. The cell medium in well was aspirated after 36 h of incubation with the polymers and cells were washed thrice properly with sterile phosphate buffer saline (PBS). Finally, 100 μ L of MTT reagent (0.5 g/L in PBS) and 100 μ L fresh media were added to each well to reduce the MTT to formazan dye by the enzyme of the live cells in each well. After 3 h of incubation, MTT was replaced with 200 μ L of DMSO in each well to solubilize the formazan dye. The amount of formazan dye produced during this reduction process by the living cells was measured spectrophotometrically at 540 nm wavelength. The experiment was performed in triplicate and an average value was taken. The cytotoxicity of the polymers was expressed as percentage of cell viability with respect to the untreated (without addition of any polymer) control cells (100% cell viable), using the following equation

$$\text{Cell viability (\%)} = (\text{Mean of absorbance value of treated cells} / \text{Mean of absorbance value of control cells}) \times 100 \quad (3)$$

2.11. Hemolysis

The hemocompatibility experiment was conducted in compliance with the relevant laws and guideline of the "Institute Ethical Committee". Polymers' hemocompatibility was checked following a standard protocol [46,47,51,52]. Stock polymer solutions were prepared in phosphate buffer saline (PBS) of pH 7.4 and incubated for minimum 6 h. Approximately 5 mL of fresh human blood were taken from a healthy volunteer with consent before the experiment and red blood cells (RBCs) were procured from the collected human blood by centrifugation at 3000 rpm for 10 min at room temperature. Then serum was decanted from the blood sample and RBCs were washed 4 times with 150 mM NaCl solution to remove the serum completely. The final RBC cell concentration ($\sim 5 \times 10^8$ RBC/mL) was prepared as suspended solution in PBS. Then 200 μ L of the final RBC suspension was mixed properly with the desired amount of polymer and PBS of pH 7.4 to make 1 mL mixture of different polymer concentrations. Negative and positive control for this measurement were RBC cells suspension in only PBS and RBC cells suspension mixed with triton X-100 (1%, w/v) respectively. All these samples as well as the controls in the micro-centrifuge tubes were incubated for 60 min at 310 K in water bath with an intermittent mixing and then were centrifuged at 12,000 rpm for 5 min to separate unperturbed RBC cells from the solution. The supernatants were collected from each sample to check their absorbance values at 541 nm in ELISA reader (Biorad, USA) using PBS as the blank. The study was repeated in triplicate and an average was taken for each polymer concentration.

3. Results and discussions

3.1. Molecular characterization

The structure of the monomer and anionic polymers (APs) was identified by ¹H and ¹³C NMR spectra (Figs. S1–S4). The mole ratio

of HEMA-DTDPA and mPEG in the copolymer was determined from the corresponding peak intensities in the respective ^1H NMR spectrum (Figs. S3 and S4) and were observed to be 1:2 and 1:4 for **AP12** and **AP14**, respectively. Thus, **AP12** has more number of $-\text{COO}^-$ groups and $-\text{S}-\text{S}-$ linkages in the polymer in comparison to those of **AP14**. The M_w of the copolymers obtained from GPC measurements (Fig. S5) are 34,723 and 23,500 for **AP12** and **AP14**, respectively. The PDI values of the copolymers **AP12** (1.48) and **AP14** (1.43) were observed to be relatively low which is advantageous for drug delivery applications.

3.2. Surface activity

Both copolymers were observed to be highly soluble in water at room temperature which was indicated by the high % T value ($\sim 95\%$) even at a reasonably high concentration (1.0 mg mL^{-1}) (Fig. 1(a)). The amphiphilic character of the copolymers was examined by the surface tension measurements. Both the polymers were found to be surface active as evidenced by the surface tension plots in Fig. 1(b). Both copolymers lowered the γ value of water (pH 7) with the gradual increase of polymer concentration (C_p) at 298 K. The lowering of the γ value is a clear indication of amphiphilic nature of these copolymers. The concentration corresponding to the starting point of the plateau (indicated by upward and downward arrows) in the graph can be taken as the critical aggregation concentration (CAC) of the copolymer. The CAC value for both copolymers was observed to be equal to $\sim 10 \mu\text{g mL}^{-1}$. However, **AP12** polymer is observed to be slightly more surface active than the **AP14** polymer and can be attributed to relatively higher molecular weight of the former.

3.3. Self-assembly behaviour

The self-assembly behaviour of the copolymers were studied by steady-state fluorescence technique using hydrophobic probes NPN and Py as described in the literatures [46,47,51,52]. NPN is generally nonfluorescent in water, but its fluorescence intensity

is increased associated with a blue shift of the λ_{max} when it enters into the hydrophobic environment of any aggregate [46,47,51,52]. For both **AP12** and **AP14**, a huge blue shift ($\Delta\lambda$) of λ_{max} as ($\Delta\lambda = \lambda_{\text{polymer}} - \lambda_{\text{water}}$) with the increase in C_p was observed following a distinct sigmoid pattern of the plot ($\Delta\lambda$ vs C_p) indicating solubilization of NPN molecules within the hydrophobic microenvironments formed by the copolymers [46,47,51,52]. The fluorescence titration curves as depicted in Fig. 1(c) showed that the onset of rise (indicated by upward and downward arrows) of $\Delta\lambda$ occurs above a critical concentration (CAC) equal to $4 \mu\text{g mL}^{-1}$ for **AP12** and $6 \mu\text{g mL}^{-1}$ for **AP14**.

Fluorescence titration using Py probe was also carried out to validate the result of NPN titration. It is also nearly insoluble in water and gives very less intense spectrum in water. But Py can be solubilised in the hydrophobic core of any aggregates with an intensified fluorescence spectrum. Unlike NPN, the fluorescence spectrum of Py shows five vibronic peaks of which the ratio (I_1/I_3) of the first (I_1) and third peak (I_3) is very much sensitive to the polarity change of the medium [46,47,51,52]. With increasing solubility of the Py in the hydrophobic core of the aggregates, I_1/I_3 ratio gradually decreases with the increase of C_p (Fig. 1(d)) [46,47,51,52]. The gradual decrease of I_1/I_3 ratio of Py for the polymers with the increase of C_p confirms microstructure formation. The CAC values corresponding to the concentration of onset of fall of I_1/I_3 ratio (indicated by upward and downward arrows) are $5 \mu\text{g mL}^{-1}$ for **AP12** and $7 \mu\text{g mL}^{-1}$ for **AP14**, which within the experimental error limit, are in good agreement with the values obtained from fluorescence titrations using NPN probe. Thus it can be concluded that though the polymers have no typical hydrophobic moiety attached to the polymeric backbone, they exhibit aggregation above a relatively low CAC value.

3.4. Shape and size of aggregates

In order to visualize the microstructure of the aggregates, HRTEM images of the polymer solution (in phosphate buffer of pH 7) were taken at two different concentrations (0.2 and

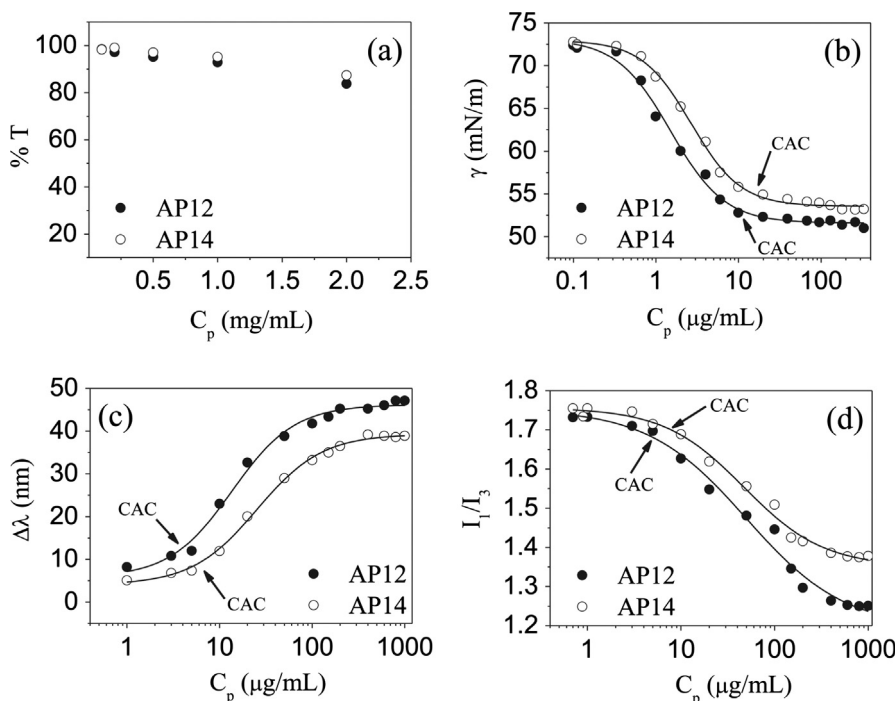


Fig. 1. Plots of (a) percent transmittance (% T), (b) γ (mN/m) of water, (c) shift ($\Delta\lambda$) of λ_{max} as ($\Delta\lambda = \lambda_{\text{polymer}} - \lambda_{\text{water}}$) of NPN and (d) intensity ratio (I_1/I_3) of Py fluorescence as a function of C_p in pH 7 buffer at 298 K.

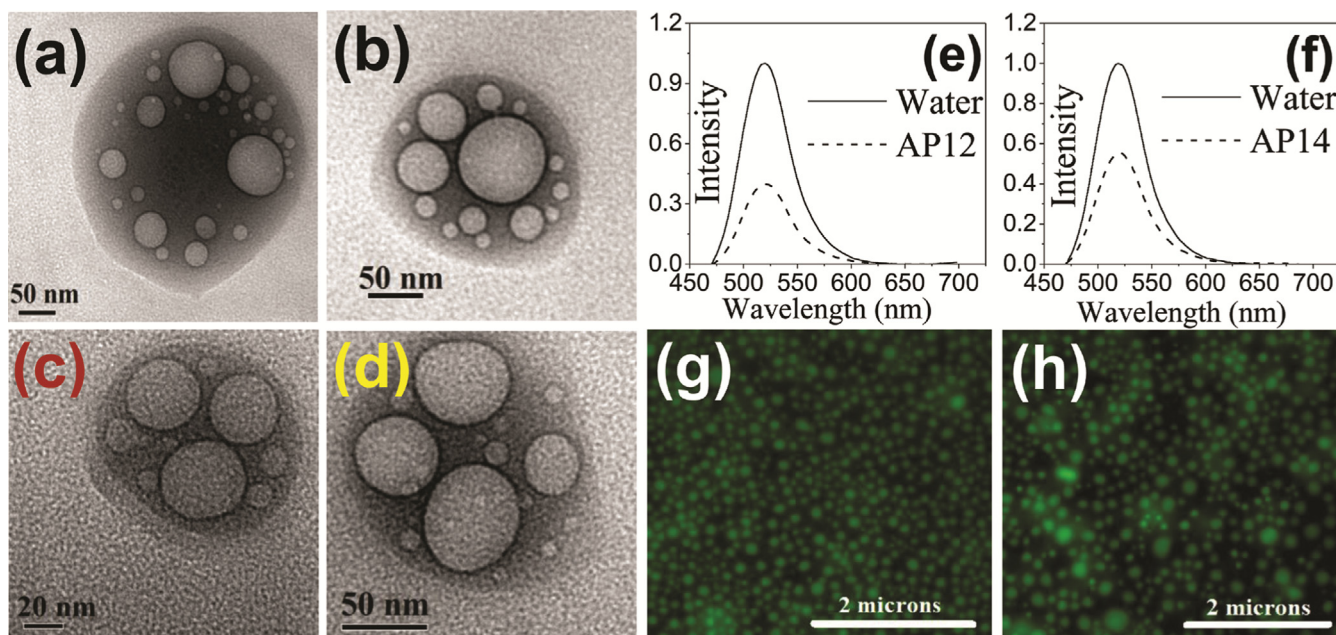


Fig. 2. Unstained HRTEM images (a, b, c, d) of polymeric aggregates in solutions containing 0.2 mg mL^{-1} (a, c) and 1.0 mg mL^{-1} (b, d) **AP12** (a, b) and **AP14** (c, d) copolymers at 298 K; Normalized fluorescence spectrum of Cal in aqueous buffers (pH 7) in absence (control) and presence of (e) **AP12** and (f) **AP14** copolymer (0.2 mg mL^{-1}); FCM images of Cal entrapped polymersomes in solutions of (g) **AP12** and (h) **AP14**, scale bar represents $2 \mu\text{m}$.

1.0 mg mL^{-1}). The images shown in Fig. 2(a–d) reveal the existence of vesicles with inner diameter (i.d.) in the range of 20–80 nm in solutions of both the polymers. However, the majority of the vesicles have i.d. less than ca. 100 nm. It should be noted that the micrographs in Fig. 2(a–d) show only the presence of unilamellar vesicles.

Since conventional TEM experiment involves drying of the sample, the morphology of the self-assembled structures is often criticised in the literature. However, the TEM pictures as shown in Fig. 2(a–d) were reproducible. To further support the existence of aqueous core within the aggregates, hydrophilic dye (Cal) entrapment experiment was performed with the solutions of both copolymers following previous literatures [46,47,57]. Figs. 2(e, f) show that the intensity of normalized fluorescence spectrum of Cal in the presence of either **AP12** or **AP14** polymer is much less relative to the intensity of fluorescence spectrum of the absorbance-matched Cal solution in pure buffer. This self-quenching of the Cal fluorescence is a result of confinement of Cal molecules in the small aqueous core of vesicles, confirming polymersome formation by these two anionic copolymers in pH 7 buffer [46,47,57]. The presence of the vesicular aggregates can be further visualized in the confocal fluorescence microscopic images (Fig. 2(g, h)) of the Cal-entrapped polymersomes in solutions of both polymers. The observation of green spots upon excitation of the samples clearly proves the existence of Cal in the aqueous core of the vesicular aggregates [24]. The average i.d. of these vesicles is in the range of ca. 100–150 nm.

Hydrodynamic diameter (d_H) of the self-assembled polymeric vesicles was also measured using DLS technique. The size distribution profiles obtained at different concentrations of both **AP12** and **AP14** polymers are displayed in Fig. 3(a, b). Only monomodal size distribution at lower concentrations ($\leq 0.5 \text{ mg mL}^{-1}$) can be observed with both polymers. However, at higher concentrations (e.g., 1.0 mg mL^{-1}) a bimodal size distribution for both the polymers can be seen in Fig. 3(a, b). Although smaller aggregates of mean d_H of 3–5 nm can be observed, the majority of aggregates are observed to have mean d_H in the range of 110–140 nm consistent with vesicular structures. Thus the mean hydrodynamic size

of the polymersomes is closely equal to those obtained from fluorescence microscopic images. The polymersomes have ideal size required for intravenous DDS [58]. The polydispersity of the vesicle size is a consequence of the polydispersed sample of the copolymers.

In order to determine surface charge of the polymersomes, zeta potential was measured at different polymer concentrations in aqueous media (pH 7) at 298 K. The bar graphs in Fig. 4 show that zeta potential values are negative at pH 7 for both the polymers at all concentrations. Significant negative zeta potential values of the polymersomes confirm that the corona of the vesicles is composed of the ionized DTDPA moieties containing $-\text{COOH}$ groups. In other words, the mPEG chains form the bilayer membrane of the polymersome (Scheme 1). This is similar to their high-molecular-weight analogues [46,47] as well as to low-molecular-weight surfactant monomers [48–50].

The absence of appearance of any turbidity or phase separation (Fig. S6) for a given concentration (1.0 mg mL^{-1}) of the polymer at different temperatures (298–333 K) is consistent with the fact that the mPEG chains constitute the bilayer membrane of the polymersomes as shown in Scheme 1.

3.5. pH-Triggered dye release

pH is an important stimulus for triggering release of encapsulated drug molecules at the target site, especially at the tumor site having acidic environment. The above discussion suggests that the polymersomes have $-\text{COO}^-$ groups on their surface, which are sensitive to the pH change of the medium. The reduction of the solution pH causes protonation of the $-\text{COO}^-$ groups and thereby destabilizes the bilayer vesicles and a burst release of the encapsulated drug occurs. Even if the polymersomes remain intact in acidic medium, the hydrolysis of ester linkages in the polymer side chain can destabilize the membrane facilitating slow release of the entrapped drug molecules due to enhanced diffusion. Thus pH-responsive release of the polymersome encapsulated guest was studied using a pH-sensitive hydrophilic dye Cal (model drug), following a standard protocol reported in literature, as its

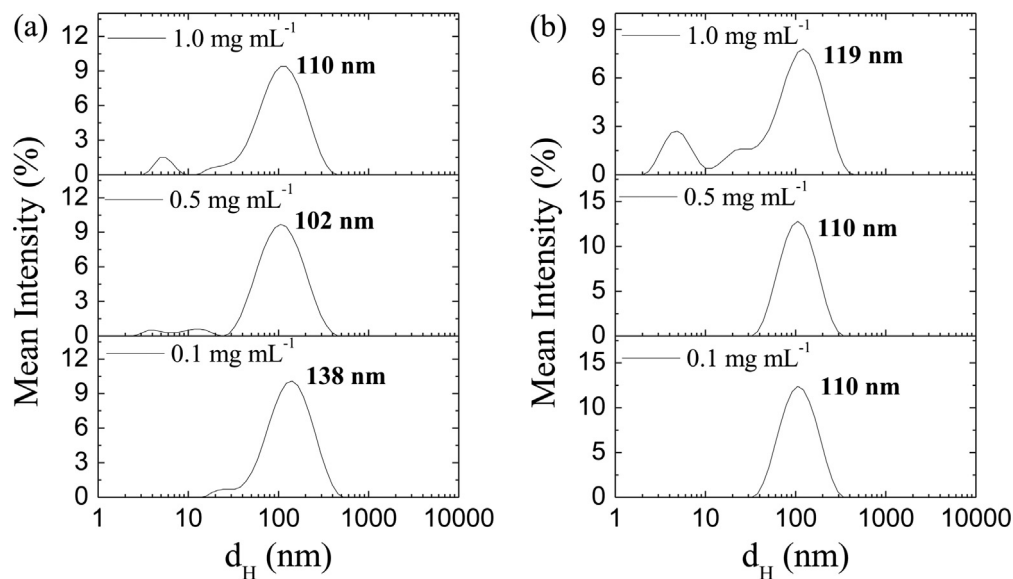


Fig. 3. Hydrodynamic size distributions of aggregates in buffer (pH 7) solutions of (a) AP12 and (b) AP14 copolymers at different concentrations at 298 K.

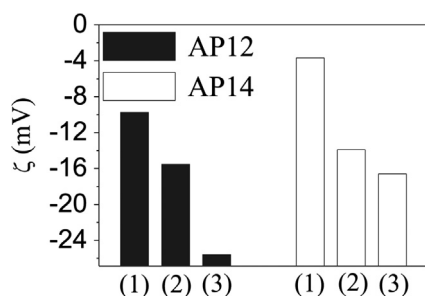
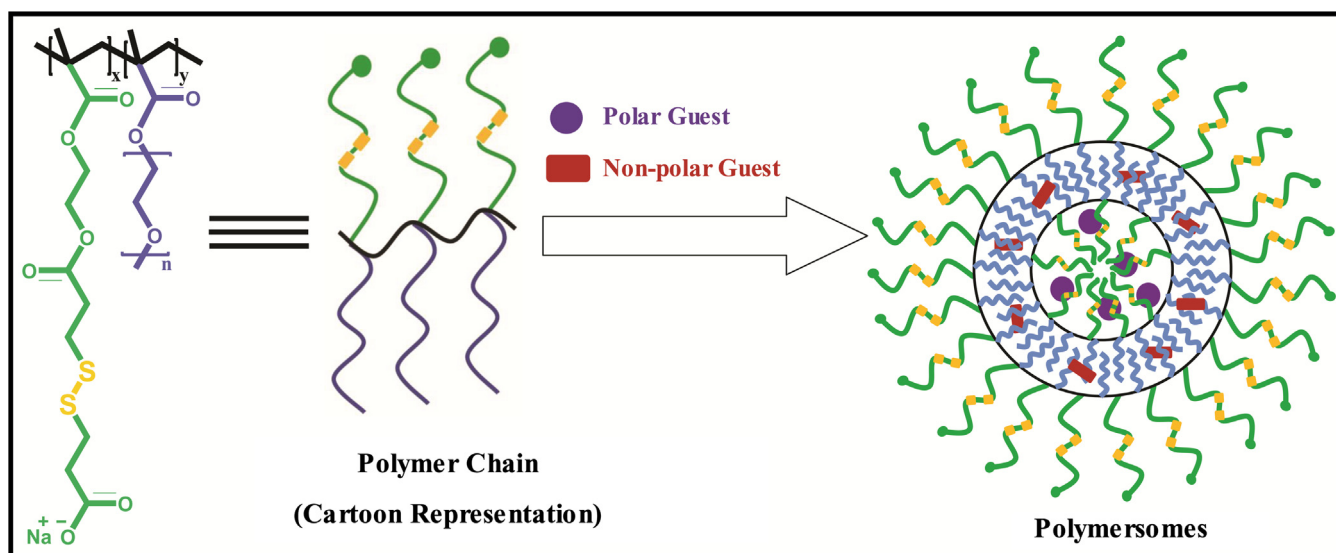


Fig. 4. Bar graphs showing zeta potential (ζ mV) values at different concentrations ((1) 0.1 mg mL⁻¹, (2) 0.5 mg mL⁻¹, (3) 1.0 mg mL⁻¹) of AP12 and AP14 copolymers in buffer (pH 7) at 298 K.

fluorescence intensity is known to decrease with the increase as well as decrease of pH of the medium [46,47,59]. So, after successful encapsulation of Cal by these anionic polymersomes, the

release of the guest was observed by measuring its fluorescence intensity at different pHs. The fluorescence spectra depicted in Fig. 5(a, b) show a gradual decrease of fluorescence intensity of the encapsulated Cal with the decrease of pH of the medium after 30 min of incubation. This gradual reduction of fluorescence intensity confirms the release of Cal dye from the aqueous core of the polymersomes into the bulk water of acidic pH. The observation of burst release (~40–45%) of Cal from the polymersomes also confirms release of the guest molecule due to the protonation of the $-\text{COO}^-$ groups of the polymers and not due to the slow hydrolysis of the ester bonds.

The aqueous solubility of the polymers at different pH was also determined by measuring turbidity of the solutions at room temperature (298 K). The plots in Fig. S7 show that both polymers produce clear solution in water at pH > 6.0 as indicated by the higher % T value. However, % T value starts to fall as the pH is gradually decreased below 6.0. At pH below 4, the solution for AP12 becomes turbid indicating complete protonation of the $-\text{COO}^-$ groups. Therefore, the pH corresponding to the 50% T can



Scheme 1. Schematic representation of vesicle formation by AP12 or AP14 anionic copolymers.

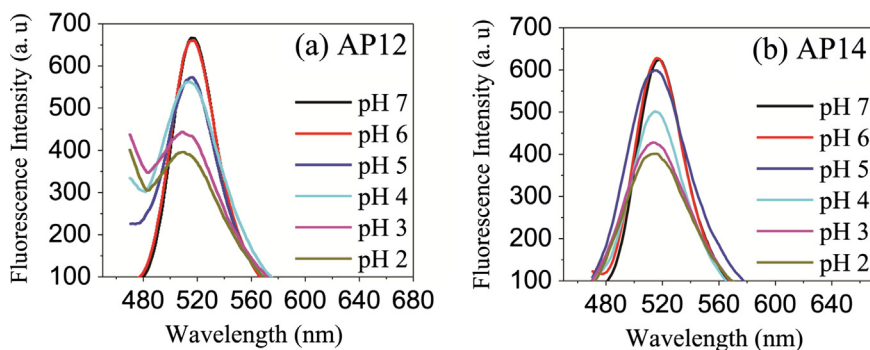


Fig. 5. Fluorescence spectra of Cal encapsulated polymersomes in solutions ($C_p = 0.2 \text{ mg mL}^{-1}$) of AP12 and AP14 copolymers at different pH at 298 K.

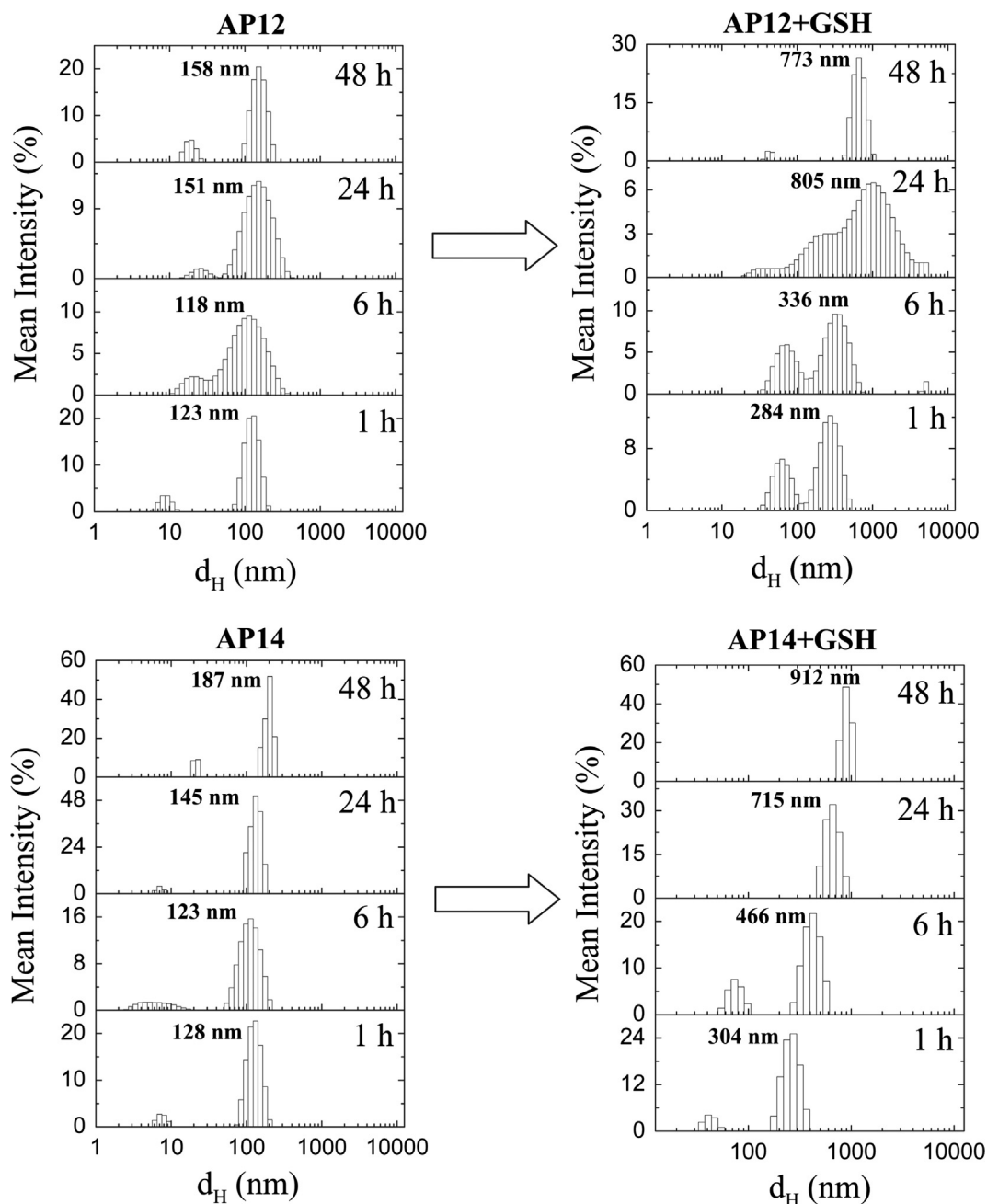


Fig. 6. Size distribution histograms in solution (0.2 mg mL^{-1} , pH 7) of AP12 and AP14 in the absence and presence of GSH (10 mM) at different time intervals at 298 K.

be taken as the pK_a of the $-\text{COOH}$ group. Although the solution of **AP12** polymer becomes turbid at pH 5 and turbidity reached nearly 100% at pH 4 (Fig. S7), but the polymer did not precipitate out from the solution as the protonated polymer is a liquid at room temperature. This means the polymer forms a stable emulsion in acidic pH. On the other hand, the solution of **AP14** does not exhibit any turbidity in the pH range of 2–9. This is because for **AP14**, the contents of HEMA-DTDPA moiety containing $-\text{COOH}$ group and mPEG chain are respectively lower and higher than that of **AP12** polymer. The greater solubility of the protonated uncharged **AP14** polymer could also be due to its low molecular weight compared to **AP14**.

3.6. Redox-sensitive disruption of polymersomes

The polymer structure (Chart 1) shows that the hydrophilic units are covalently bonded to polymer backbone through the $-\text{S}-\text{S}-$ linkage. In aqueous solution of the polymers or in the vesicular structure, these $-\text{S}-\text{S}-$ linkages are exposed to bulk water and therefore are expected to undergo redox reaction in the presence of GSH. Therefore, thiol-responsive disruption of the polymersomes and consequent release of the guest was studied using DLS and steady-state fluorescence techniques. As the polymers were observed to be more stable at pH 7.0, the measurements in the presence of GSH were performed at this pH. Hydrodynamic size distribution of the polymersomes in solutions of both **AP12** and **AP14** polymers containing 10 mM GSH was measured by DLS at different time intervals. In a control experiment, the hydrodynamic size distribution of polymersomes in the absence of GSH was also measured at the same time intervals. The results presented in Fig. 6 show a huge increase of mean d_H value of the aggregates in the presence of GSH. However, no significant change

in the mean d_H value is observed when GSH is absent in the polymer solution. This is a clear indication of disassembly of the polymersomes due to breakage of the $-\text{S}-\text{S}-$ bonds in the side chains. The increase in size of the polymers might be due to the inter-polymer $-\text{S}-\text{S}-$ bond formation leading to formation of larger polymer or polymer networks.

The dissociation of the hydrophilic units from the polymer backbone was also demonstrated by the release of fluorescent Cal dye from the aqueous core of the polymersomes in the presence of GSH. As discussed before, the fluorescence spectra of Cal showed a reduction of intensity when solubilized within the aqueous core of the polymersomes (Fig. 7(a, b)). However, it can be observed that there is a huge increase in fluorescence intensity of Cal after 10 min incubation in solution containing 10 mM GSH (Fig. 7(a, b)). The control experiment in the absence of polymer, however, did not show any change of fluorescence intensity of Cal. This clearly suggests disruption of the Cal-entrapped polymersomes due to the breakage of the $-\text{S}-\text{S}-$ linkages in presence of GSH, resulting in a burst release of Cal and subsequent increase of the fluorescent intensity (as evidenced from Fig. S8) due to dilution as reported in literature [34]. The release of the Cal dye from the polymersomes was also tested at GSH concentrations equivalent to both extracellular and intracellular conditions. The results presented in Fig. 7(c, d), show that the disruption of polymersomes occurs more rapidly at the highest GSH concentration level that is under intracellular condition.

Further, HRTEM images of the polymeric solutions were taken in the presence of GSH at different time intervals to validate disintegration of the polymersomes. Copolymer solutions (0.2 mg mL^{-1}) incubated for 1 h and 12 h with 10 mM GSH and then were drop cast on the carbon coated copper grid. The images in Fig. S9(a, c)

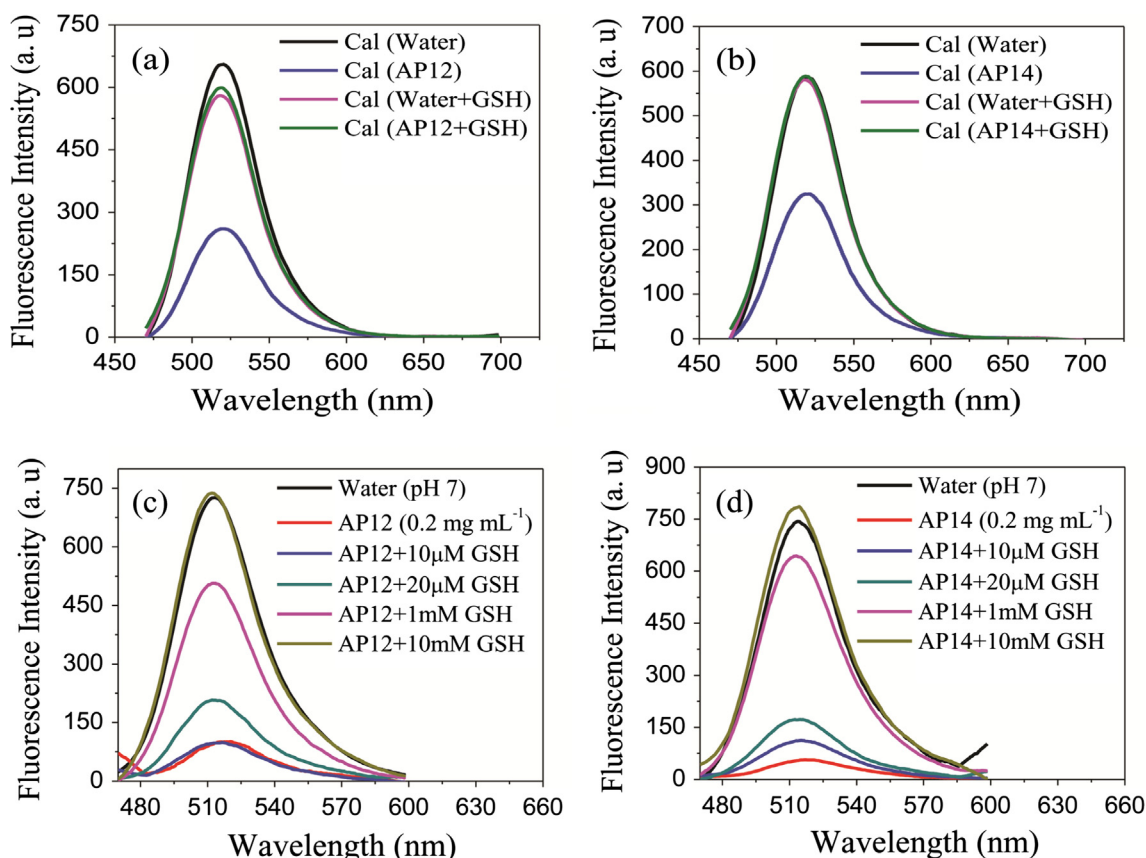


Fig. 7. Fluorescence spectra of Cal in pH 7 buffer at 298 K in the absence and presence of (a) **AP12** and (b) **AP14** polymers (0.2 mg mL^{-1}) with and without GSH (10 mM); fluorescence spectra of Cal encapsulated polymersome in solutions of (c) **AP12** and (d) **AP14** before and after the release induced by different concentrations of GSH.

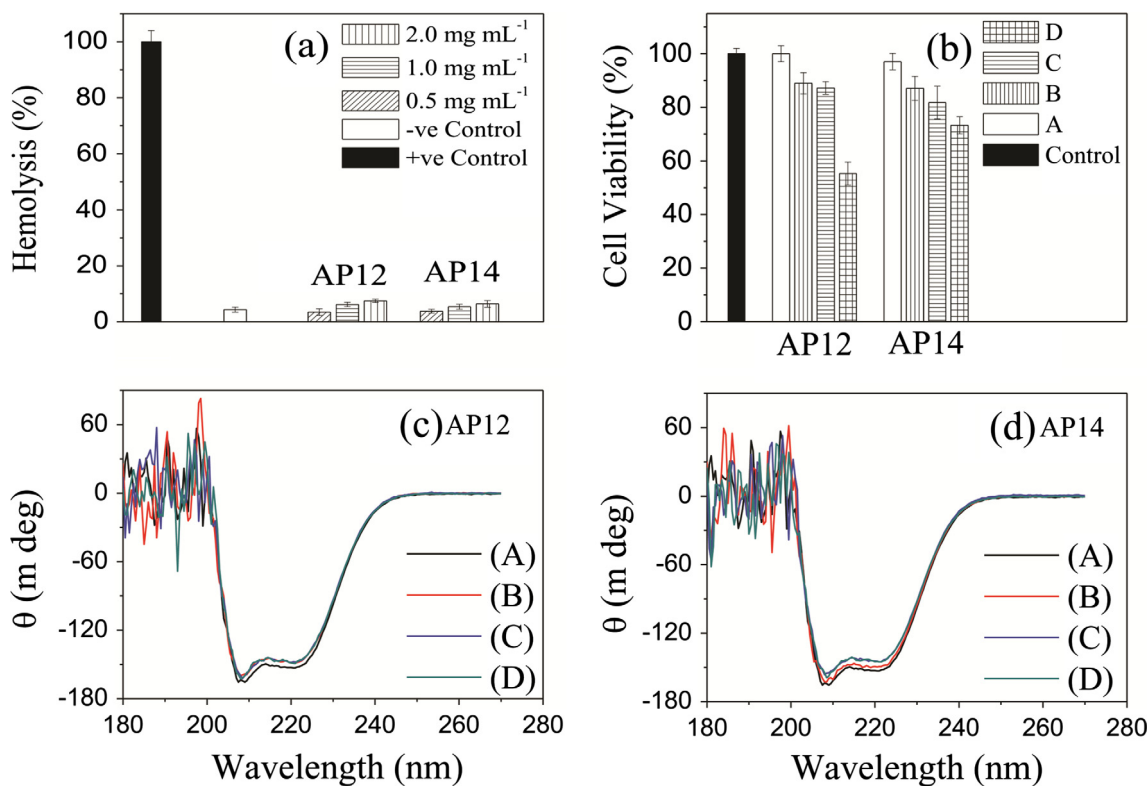


Fig. 8. (a) Bar graphs showing hemolysis (%) in the presence of **AP12** and **AP14** polymers at different concentrations (0.5, 1.0 and 2.0 mg mL⁻¹) at physiological pH (7.4); (b) Bar graphs showing cell viability (%) of the polymers on cervical cancer cells (HeLa cells) at different concentrations after incubation for 36 h: (A) 0.1, (B) 0.02, (C) 0.5, and (D) 1.0 mg mL⁻¹; CD spectra of HSA (0.1%, w/v) in PBS buffer (20 mM, pH 7.0) in the absence and presence of different concentrations of (c) **AP12** and (d) **AP14** polymers at 298 K: (A) 0.0 mg mL⁻¹, (B) 0.1 mg mL⁻¹, (C) 0.5 mg mL⁻¹, and (D) 1.0 mg mL⁻¹.

clearly indicate disruption of the vesicle structures in the presence of GSH within 1 h. The solutions after 12 h of incubation, on the other hand, do not reveal any specific aggregate, except some featureless microstructures (Fig. S9(b, d)).

3.7. In vitro cytotoxicity studies

For application as drug delivery vehicles, polymers should be nontoxic within the therapeutic window of the drug. In addition, for use as injectable DDS, the polymer should also be hemocompatible. Therefore, hemolysis study using these polymers from a low to high concentration range (0.1, 0.5 and 1.0 mg mL⁻¹) was carried out. The results presented in Fig. 8(a) show that none of the polymers exhibits any hemolysis at the concentrations employed. Though **AP12** is slightly less hemocompatible than **AP14**, both these hemocompatible polymers can be used in intravenous drug delivery. For the cell viability test, HeLa cells were treated with the polymers of varying concentrations (0.1, 0.2, 0.5 and 1.0 mg mL⁻¹) for 36 h and the results are summarized in Fig. 8(b). It is observed that there is 90% cell viability even at the concentration of 0.5 mg mL⁻¹ for both the polymers. However, at the highest concentration (1.0 mg mL⁻¹), both the polymers showed relatively less viability and **AP12** polymer was found to be more toxic than **AP14** probably due to low mPEG content of the former polymer. Overall, both these cell viable polymers can be employed up to a relatively high concentration and can therefore be considered for drug delivery applications.

3.8. Interaction of polymers with HSA

HSA is the most abundant circulatory protein in human blood and is responsible for the transport of various fatty acids,

metabolites, and drug molecules [53]. Therefore, the interaction of HSA with any DDS is important, especially with injectable ones. To monitor the changes in structure, conformation, and stability of the protein in solution, CD spectra were measured in the absence as well as in the presence of both polymers [53–56]. The CD spectrum (Fig. 8(c, d)) of HSA exhibits negative minima at 208 and 222 nm, indicating the presence of the α -helix structure of this circulatory protein [53–56]. However, in the presence of **AP12** or **AP14** polymers the CD spectrum shows a slight decrease in band intensity at both 208 and 222 nm wavelengths without any shift of the peaks, indicating a slight decrease in the helical structure content of the protein (Table S1). This means HSA can carry these polymeric nanocarriers to their site of action without any damage to its secondary structure.

4. Conclusions

In summary, two dual stimuli-sensitive mPEG-based polymers containing different amounts of acidic functionality were synthesized using comparatively very easy random polymerization technique. These water-soluble polymers spontaneously formed anionic vesicles in pH 7 buffer at room temperature. In fact, this is one of the few reports on polymersome formation by random copolymers [46,47]. Further it is important to note that unlike most reports [43–45], these polymersomes were produced without the help of any external stimulus. Like zwitterionic and cationic polymersomes or low molecular weight cationic and zwitterionic vesicular aggregates [46–49], here also the moieties containing the anionic (–COO⁻) head groups project themselves towards water and mPEG chains constitute the bilayer membrane of the vesicles. In most polymeric aggregates reported in literature [33–38], have S–S linkages in the interior of aggregate structure,

but in these redox-active polymersomes, the S–S linkages are exposed to the bulk aqueous environment. The polymersomes were observed to encapsulate hydrophilic as well as hydrophobic guest molecules in their aqueous core and bilayer membrane, respectively. The polymersomes were found to be stable at body temperature (37 °C) avoiding the possibility of any premature release of guest molecules. These anionic polymersomes were observed to exhibit pH- and redox-sensitive disassembly with the concomitant release of the guest molecules. Due to their redox-sensitive nature, they are also smarter drug delivery systems than our previously reported zwitterionic polymersomes [46] or any other anionic polymersomes. Unlike **AP14**, the **AP12** polymer produces stable self-emulsion on lowering of the pH below 4. Thus, **AP14** is more acceptable as pH-responsive drug delivery carrier than **AP12**. Their high hemocompatibility and cell viability is beneficial for the development of better delivery systems. Further, they were not found to destabilize the secondary structure of the circulatory protein, HSA. Thus it can be concluded that these anionic dual stimuli-sensitive, biocompatible, and stable polymersomes can have potential application as intravenous drug delivery systems for cancer chemotherapy.

Acknowledgements

The authors gratefully acknowledge the Department of Science and Technology, New Delhi for the financial support (Grant no. SR/S1/PC-68/2008) of this work. PL thanks CSIR, New Delhi (no. 20-06/2010 (i) EU-IV) for a research fellowship. The assistance with the cell viability measurements by Mr. Devdeep Mukhopadhyay, Department of Biotechnology is sincerely acknowledged.

Appendix A. Supplementary material

Supplementary data associated with this article can be found, in the online version, at <http://dx.doi.org/10.1016/j.jcis.2017.04.034>.

References

- [1] A.P. Johnston, G.K. Such, S.L. Ng, F. Caruso, Challenges facing colloidal delivery systems: from synthesis to the clinic, *Curr. Opin. Colloid Interface Sci.* 16 (2011) 171–181.
- [2] W.B. Liechty, D.R. Kryscio, B.V. Slaughter, N.A. Peppas, Polymers for drug delivery systems, *Annu. Rev. Chem. Biomol. Eng.* 1 (2010) 149–173.
- [3] R. Tong, L. Tang, L. Ma, C. Tu, R. Baumgartner, J. Cheng, Smart chemistry in polymeric nanomedicine, *Chem. Soc. Rev.* 43 (2014) 6982–7012.
- [4] C. Zhu, L. Liu, Q. Yang, F. Lv, S. Wang, Water-soluble conjugated polymers for imaging, diagnosis, and therapy, *Chem. Rev.* 112 (2012) 4687–4735.
- [5] G.S. Kwon, T. Okano, Polymeric micelles as new drug carriers, *Adv. Drug Deliv. Rev.* 21 (1996) 107–116.
- [6] J.S. Lee, J. Feijen, Polymersomes for drug delivery: design, formation and characterization, *J. Control. Release* 161 (2012) 473–483.
- [7] E.R. Gillies, J.M. Frechet, Dendrimers and dendritic polymers in drug delivery, *Drug Discov. Today* 10 (2005) 35–43.
- [8] F. Meng, Z. Zhong, J. Feijen, Stimuli-responsive polymersomes for programmed drug delivery, *Biomacromol* 10 (2009) 197–209.
- [9] D.A. Christian, S. Cai, D.M. Bowen, Y. Kim, J.D. Pajeroski, D.E. Discher, Polymersome carriers: from self-assembly to siRNA and protein therapeutics, *Eur. J. Pharm. Biopharm.* 71 (2009) 463–474.
- [10] P. Tanner, S. Egli, V. Balasubramanian, O. Onaca, C.G. Paliwan, W. Meier, Can polymeric vesicles that confine enzymatic reactions act as simplified organelles?, *FEBS Lett* 585 (2011) 1699–1706.
- [11] G. Battaglia, A.J. Ryan, Bilayers and interdigitation in block copolymer vesicles, *J. Am. Chem. Soc.* 127 (2005) 8757–8764.
- [12] H. Bermudez, A.K. Brannan, D.A. Hammer, F.S. Bates, D.E. Discher, Molecular weight dependence of polymersome membrane structure, elasticity, and stability, *Macromolecules* 35 (2002) 8203–8208.
- [13] U. Borchert, U. Lipprandt, M. Bilang, A. Kimpfler, A. Rank, R. Peschka-Süss, S. Förster, PH-induced release from P2VP-PEO block copolymer vesicles, *Langmuir* 22 (2006) 5843–5847.
- [14] M.A.C. Stuart, W.T. Huck, J. Genzer, M. Müller, C. Ober, M. Stamm, G.B. Sukhorukov, I. Szleifer, V.V. Tsukruk, M. Urban, F. Winnik, Emerging applications of stimuli-responsive polymer materials, *Nat. Mater.* 9 (2010) 101–113.
- [15] A. Kumar, A. Srivastava, I.Y. Galaev, B. Mattiasson, Smart polymers: physical forms and bioengineering applications, *Prog. Polym. Sci.* 32 (2007) 1205–1237.
- [16] K.M. Huh, H.C. Kang, Y.J. Lee, Y.H. Bae, PH-sensitive polymers for drug delivery, *Macromol. Res.* 20 (2012) 224–233.
- [17] S. Kumar, P. De, Fluorescent labelled dual-stimuli (pH/thermo) responsive self-assembled side-chain amino acid based polymers, *Polymer* 55 (2014) 824–832.
- [18] S.D. Fitzpatrick, L.E. Fitzpatrick, A. Thakur, M.A.J. Mazumder, H. Sheardown, Temperature-sensitive polymers for drug delivery, *Expert Rev. Med. Dev.* 9 (2012) 339–351.
- [19] B. Maiti, S. Maiti, P. De, Self-assembly of well-defined fatty acid based amphiphilic thermoresponsive random copolymers, *RSC Adv.* 6 (2016) 19322–19330.
- [20] H. Cho, J. Bae, V.K. Garripelli, J.M. Anderson, H.W. Jun, S. Jo, Redox-sensitive polymeric nanoparticles for drug delivery, *Chem. Commun.* 48 (2012) 6043–6045.
- [21] T.Y. Liu, S.H. Hu, K.H. Liu, R.S. Shaiu, D.M. Liu, S.Y. Chen, Instantaneous drug delivery of magnetic/thermally sensitive nanospheres by a high-frequency magnetic field, *Langmuir* 24 (2008) 13306–13311.
- [22] C. Alvarez-Lorenzo, L. Bromberg, A. Concheiro, Light-sensitive intelligent drug delivery systems, *Photochem. Photobiol.* 85 (2009) 848–860.
- [23] W.G. Pitt, G.A. Hussein, B.J. Staples, Ultrasonic drug delivery—a general review, *Exp. Opin. Drug Deliv.* 1 (2004) 37–56.
- [24] S. Haas, N. Hain, M. Raoufi, S. Handschuh-Wang, T. Wang, X. Jiang, H. Schönherr, Enzyme degradable polymersomes from hyaluronic acid-block-poly (ϵ -caprolactone) copolymers for the detection of enzymes of pathogenic bacteria, *Biomacromol* 16 (2015) 832–841.
- [25] J. Zhang, L. Wu, F. Meng, Z. Wang, C. Deng, H. Liu, Z. Zhong, PH and reduction dual-bioresponsive polymersomes for efficient intracellular protein delivery, *Langmuir* 28 (2011) 2056–2065.
- [26] R.A. Cairns, I.S. Harris, T.W. Mak, Regulation of cancer cell metabolism, *Nat. Rev. Cancer* 11 (2011) 85–95.
- [27] W. Gao, J.M. Chan, O.C. Farokhzad, PH-responsive nanoparticles for drug delivery, *Mol. Pharm.* 7 (2010) 1913–1920.
- [28] W. Cheng, J.N. Kumar, Y. Zhang, Y. Liu, PH-and redox-responsive poly (ethylene glycol) and cholesterol-conjugated poly (amido amine) s based micelles for controlled drug delivery, *Macromol. Biosci.* 14 (2014) 347–358.
- [29] D. Schmaljohann, Thermo-and pH-responsive polymers in drug delivery, *Adv. Drug Deliv. Rev.* 58 (2006) 1655–1670.
- [30] P. Bawa, V. Pillay, Y.E. Choonara, L.C. du Toit, Stimuli-responsive polymers and their applications in drug delivery, *Biomed. Mater.* 4 (2009) 022001.
- [31] J.O. You, D. Almeda, J.C. George, D.T. Auguste, Bioresponsive matrices in drug delivery, *J. Biol. Eng.* 4 (2010) 1–12.
- [32] D.A. Christian, O.B. Garbuzenko, T. Minko, D.E. Discher, Polymer vesicles with a red cell-like surface charge: microvascular imaging and in vivo tracking with near-infrared fluorescence, *Macromol. Rapid Commun.* 31 (2010) 135–141.
- [33] V. Bulmus, M. Woodward, L. Lin, N. Murthy, P. Stayton, A. Hoffman, A new pH-responsive and glutathione-reactive, endosomal membrane-disruptive polymeric carrier for intracellular delivery of biomolecular drugs, *J. Control. Release* 93 (2003) 105–120.
- [34] S. Cerritelli, D. Velluto, J.A. Hubbell, PEG-SS-PPS: reduction-sensitive disulfide block copolymer vesicles for intracellular drug delivery, *Biomacromol* 8 (2007) 1966–1972.
- [35] L. Jia, D. Cui, J. Bignon, A. Di Cicco, J. Wdzieczak-Bakala, J. Liu, M.H. Li, Reduction-responsive cholesterol-based block copolymer vesicles for drug delivery, *Biomacromol* 15 (2014) 2206–2217.
- [36] B. Khorasand, G. Lapointe, C. Brett, J.K. Oh, Intracellular drug delivery nanocarriers of glutathione-responsive degradable block copolymers having pendant disulfide linkages, *Biomacromol* 14 (2013) 2103–2111.
- [37] M. Huo, J. Yuan, L. Tao, Y. Wei, Redox-responsive polymers for drug delivery: from molecular design to applications, *Polym. Chem.* 5 (2014) 1519–1528.
- [38] R.Q. Li, Y. Hu, B.R. Yu, N.N. Zhao, F.J. Xu, Bioreducible comb-shaped conjugates composed of secondary amine and hydroxyl group-containing backbones and disulfide-linked side chains with tertiary amine groups for facilitating gene delivery, *Bioconjugate Chem.* 25 (2013) 155–164.
- [39] L. Sun, J. Liu, H. Zhao, Reactive polymeric micelles with disulfide groups in the coronae, *Polym. Chem.* 5 (2014) 6584–6592.
- [40] S.H. Lee, M.K. Gupta, J.B. Bang, H. Bae, H.J. Sung, Current progress in reactive oxygen species (ROS)-responsive materials for biomedical applications, *Adv. Healthc. Mater.* 2 (2013) 908–915.
- [41] B.M. Discher, Y.Y. Won, D.S. Ege, J.C. Lee, F.S. Bates, D.E. Discher, D.A. Hammer, Polymersomes: tough vesicles made from diblock copolymers, *Science* 284 (1999) 1143–1146.
- [42] D.E. Discher, F. Ahmed, Polymersomes, *Annu. Rev. Biomed. Eng.* 8 (2006) 323–341.
- [43] F. Meng, C. Hiemstra, G.H. Engbers, J. Feijen, Biodegradable polymersomes, *Macromolecules* 36 (2003) 3004–3006.
- [44] V.A. Vasantha, S. Jana, S.S.C. Lee, C.S. Lim, S.L.M. Teo, A. Parthiban, J.G. Vancso, Dual hydrophilic and salt responsive schizoprenic block copolymers—synthesis and study of self-assembly behavior, *Polym. Chem.* 6 (2015) 599–606.
- [45] J. Zhou, F. Ke, Y.Y. Tong, Z.C. Li, D. Liang, Solution behavior of copolymers with poly (ethylene oxide) as the “hydrophobic” block, *Soft Matter* 7 (2011) 9956–9961.

- [46] P. Laskar, J. Dey, S.K. Ghosh, Spontaneous polymersome formation by pH-responsive and biocompatible random copolymers as drug delivery systems, *Colloids Surf. B* 139 (2015) 107–116.
- [47] P. Laskar, J. Dey, P. Banik, M. Mandal, S.K. Ghosh, In vitro drug and gene delivery using random cationic copolymers forming stable and pH-sensitive polymersomes, *Macromol. Biosci.* (2016), <http://dx.doi.org/10.1002/mabi.201600324>.
- [48] R. Ghosh, J. Dey, Vesicle formation by l-cysteine-derived unconventional single-tailed amphiphiles in water: A fluorescence, microscopy, and calorimetric investigation, *Langmuir* 30 (2014) 13516–13524.
- [49] J. Dey, S. Shrivastava, Physicochemical characterization and self-assembly studies on cationic surfactants bearing mPEG tail, *Langmuir* 28 (2012) 17247–17255.
- [50] J. Dey, S. Shrivastava, Can molecules with an anionic head and a poly (ethylene glycol) methyl ether tail self-assemble in water? A surface tension, fluorescence probe, light scattering, and transmission electron microscopic investigation, *Soft Matter* 8 (2012) 1305–1308.
- [51] P. Laskar, S. Samanta, S.K. Ghosh, J. Dey, In vitro evaluation of pH-sensitive cholesterol-containing stable polymeric micelles for delivery of camptothecin, *J. Colloid Interface Sci.* 430 (2014) 305–314.
- [52] P. Laskar, B. Saha, S.K. Ghosh, J. Dey, PEG based random copolymer micelles as drug carriers: the effect of hydrophobe content on drug solubilization and cytotoxicity, *RSC Adv.* 5 (2015) 16265–16276.
- [53] D. Bajani, P. Laskar, J. Dey, Spontaneously formed robust steroidal vesicles: physicochemical characterization and interaction with HSA, *J. Phy. Chem. B* 118 (2014) 4561–4570.
- [54] H.X. Zhang, E. Liu, Binding behavior of DEHP to albumin: spectroscopic investigation, *J. Incl. Phenom. Macrocy. Chem.* 74 (2012) 231–238.
- [55] U. Anand, C. Jash, S. Mukherjee, Spectroscopic probing of the microenvironment in a protein–surfactant assembly, *J. Phys. Chem. B* 114 (2010) 15839–15845.
- [56] E. Froehlich, J.S. Mandeville, C.J. Jennings, R. Sedaghat-Herati, H.A. Tajmir-Riahi, Dendrimers bind human serum albumin, *J. Phy. Chem. B* 113 (2009) 6986–6993.
- [57] E.N. Savariar, S.V. Aathimanikandan, S. Thayumanavan, Supramolecular assemblies from amphiphilic homopolymers: testing the scope, *J. Am. Chem. Soc.* 128 (2006) 16224–16230.
- [58] G. Storm, S. Belliot, T. Daemen, D. Lasic, Surface modification of nanoparticles to oppose uptake by the mononuclear phagocyte system, *Adv. Drug Deliv. Rev.* 17 (1995) 31–48.
- [59] B. Maherani, E. Arab-Tehrany, A. Kheiriloomoom, D. Geny, M. Linder, Calcein release behavior from liposomal bilayer; influence of physicochemical/mechanical/structural properties of lipids, *Biochimie* 95 (2013) 2018–2033.